

X-ray Imaging for Non-Destructive Microstructure Analysis at SSRF

Rongchang Chen, Ping Liu, Tiqiao Xiao,* and Lisa X. Xu*

X-ray imaging has become an essential detection technique in a wide range of research fields since its discovery by Röntgen in 1895. Up to now, X-ray tube source based imaging systems have been widely used. However, limitations arise from insufficient spatial and temporal resolution, and low contrast of these systems, which are unavoidable drawbacks. The availability of third generation synchrotron radiation (SR) facilities since the 1990s sheds light on the advancement of X-ray imaging. The high intensity, high coherence, quasi-parallel, and monochromatic characteristics of SR beams have enabled the development of SR-based high spatial and temporal X-ray imaging techniques. In the past decades, experiments have demonstrated the advantage of SR X-ray imaging in the fields of material sciences^[1] and biomedicine.^[2]

The Shanghai Synchrotron Radiation Facility (SSRF) is a third-generation synchrotron radiation light source, and it provides a powerful technical platform for scientific research and industrial applications for scientists in China and overseas. The X-ray imaging beamline (BL13W1) is one of the seven initial beamlines at SSRF, and was formally opened to users in May 2009. The double crystal monochromator at BL13W1 provides photon energies ranging from 8 to 72.5 keV with a beam size of ca. 45 mm × 5 mm. The beamline aims at developing and evaluating the effectiveness of SR-based imaging techniques in planar or computed tomography (CT) modalities.^[3] Several X-ray imaging methods, such as micro-tomography and quantitative imaging,^[4] have been developed and they have found extensive applications in biomedicine,^[5,6] materials science,^[7,8] and so on. The X-ray imaging methods and the statistics for user research fields at BL13W1 are shown in **Figure 1**, in which it is obvious that the beamline is mainly devoted to the materials science and biomedical fields.

R. Chen,^[†] T. Xiao
Shanghai Institute of Applied Physics
Chinese Academy of Science
Shanghai 201204, China
E-mail: tqiao@sinap.ac.cn
P. Liu,^[†] L. X. Xu
Med-X Research Institute
School of Biomedical Engineering
Shanghai Jiao Tong University
Shanghai 200030, China
E-mail: lisaxu@sjtu.edu.cn



^[†]These authors contributed equally to this work.

DOI: 10.1002/adma.201402956

1. Methodology Development

1.1. X-Ray Phase Imaging

Sufficient coherence of the SR beam allows the implementation of novel phase-sensitive X-ray imaging modalities.^[9] Phase-sensitive imaging enables the detection of structures that have different scattering and refraction properties with respect to the surrounding materials. Since the mid-1990s, new techniques have been developed for phase-sensitive X-ray imaging using synchrotron radiation, such as the interferometer method, the analyzer-based method, the grating-based method, and the propagation-based method.

At the BL13W1 beamline, X-ray propagation-based phase-contrast imaging (PPCI) was set up at the very beginning of its commissioning. No additional optics are required in the imaging geometry, similar to conventional absorption imaging except that the beam is sufficiently spatially coherent and the sample-to-detector distance (SDD) is increased.^[10] The edge-enhanced images produced by the PPCI approach are very useful, allowing for visualization of boundaries with different refraction properties. Wei et al. successfully utilized PPCI to investigate the microstructures of traditional Chinese medicines.^[11] Moreover, the phase information contained in PPCI radiographic fringes could be extracted by means of phase-retrieval, which enables the phase shift imposed on the wave by the sample to be recovered from the diffracted intensity distribution in the image plane or planes.^[12] Several phase-retrieval algorithms have been developed, including analytical methods and iterative methods. Ren et al. systematically investigated the selection of the best recording SDDs for two sets of images to achieve higher retrieval precision for the first-order Born-approximation-based phase-retrieval algorithm.^[13] When PPCI combines with CT, i.e., X-ray propagation-based phase-contrast CT (PPCT), typically hundreds or thousands of projections are taken. Chen et al. found that quantitative phase information could be recovered from a single SDD PPCT data set for a ratio object, which means the ratio of the real and imaginary parts of the complex refractive index is constant.^[4] Furthermore, a systematic comparison study of single SDD phase-retrieval algorithms by considering different object compositions and the effect of statistical and structural noise has been carried out.^[14] Liu et al. extended the validity of the phase-attenuation duality (PAD) method to PPCT of samples with hybrid compositions of both light and dense components with 60 keV synchrotron radiation, which demonstrated that PAD-based PPCT is practicable in imaging simultaneously both the weakly and strongly absorbing components.^[12] In addition, Qi et al. successfully established the grating-based imaging method with a phase grating and an absorption grating at BL13W1 at SSRF.^[15]

1.2. Computed Tomography

X-ray CT is a non-destructive technique widely used for visualizing the morphology of samples, and for assessing quantitative information in three-dimensional (3D) geometries and properties. With third generation SR sources, SR- μ CT has evolved as an increasingly acceptable and utilized technique for characterizing the 3D internal structures of samples in the fields of material and biomedical sciences, and its capability is further extended with the availability of spiral CT^[16] and local CT.^[17] The monochromatic SR beam yields reconstructed CT images free of beam-hardening artifacts and allows quantitative calibration in order to evaluate the linear attenuation coefficient distribution within the sample. Chen et al. demonstrated that SR- μ CT allows the evaluation of the linear attenuation coefficients in samples of mixed compositions, i.e., breast tissues, in their study. The obtained linear attenuation coefficient results for fat and fibrous tissue are in good agreement with published direct measurement results.^[18] Ye et al. successfully utilized SR- μ CT to investigate *Fructus Foeniculi*, a type of traditional Chinese medicine, in which the oil chamber was clearly differentiated and quantitative information, such as length, volume, and oil content, were obtained.^[19] Wang et al. used multi-energy X-ray micro-CT and data-constrained modeling to quantitatively characterize the three-dimensional structures of samples with a multi-scale from milli- to nanometers.^[20] Moreover, Chen et al. developed an SR- μ CT data processing software, PITRE, that is a freeware for supporting phase-sensitive X-ray image processing and tomography reconstruction.^[21] The PITRE_BM in the software package is a batch processing manager for PITRE. It executes a series of tasks (“jobs”), which are created via PITRE, without manual intervention.

Synchrotron-radiation-based X-ray fluorescence CT (XFCT), a complement to absorption CT, is a stimulated-emission tomography modality, which allows the elemental distributions to be reconstructed on a virtual section across the sample by various algorithms. Yang et al. successfully established an XFCT system at BL13W1 at SSRF, and the ordered-subsets expectation maximization algorithm was introduced into XFCT to speed up the data acquisition.^[22]

1.3. Applications at the BL13W1 Beamline of SSRF

SR-based X-ray imaging provides a powerful tool for many applications in material science, biomedicine, and so on. The typical applications at the BL13W1 beamline of SSRF are reviewed as follows.

Given the high quality of the beam properties, SR-imaging offers unique opportunities for non-destructive and in situ characterization of material microstructures through dynamic imaging techniques and SR- μ CT. Wang et al. studied the in situ growth behavior and morphological evolution of dendrites in solidifying a Sn–Bi alloy under direct current (DC) using the SR-imaging technique. It was found that the growth of dendrites is significantly suppressed due to the effect of Joule heating when imposing DC.^[8] Huang et al. used SR- μ CT to investigate fractures in short-carbon-fiber/epoxy composites, and the mechanical load response of short carbon fibers treated by oxidation and those untreated were compared. They found that the oxidation treatment is able to reduce the ineffective length of the fibers by about 20%, thereby improving the mechanical properties of these composites.^[23] Li et al. utilized SR- μ CT to investigate in situ the microstructure evolution and the mixed-interaction mechanisms of metal–ceramic materials during the microwave sintering process. The results indicate that there are some special mixed-interaction mechanisms, which may promote the sintering process during the microwave heating of metal–ceramic materials.^[24] Hughes et al. combined the use of SR- μ CT and scanning electron microscopy–ultramicrotomy to study the distribution of micrometer-sized inorganic particles within a polymer matrix. They demonstrated that the inorganic particles distributed in a polymeric matrix can form independent, but interpenetrating clusters of varying sizes and fractal dimensions, with the largest having a fractal dimension, of 2.36.^[7] Zhou et al. quantified the three-dimensional microstructure of soil aggregates as influenced by different long-term fertilization practices with SR- μ CT, in which the results demonstrate that organic fertilization can improve soil aggregation, while inorganic fertilization is ineffective, even after 25 years.^[25]

SR-imaging is especially useful for biomedical studies. An ideal bone tissue engineering graft should have both excellent

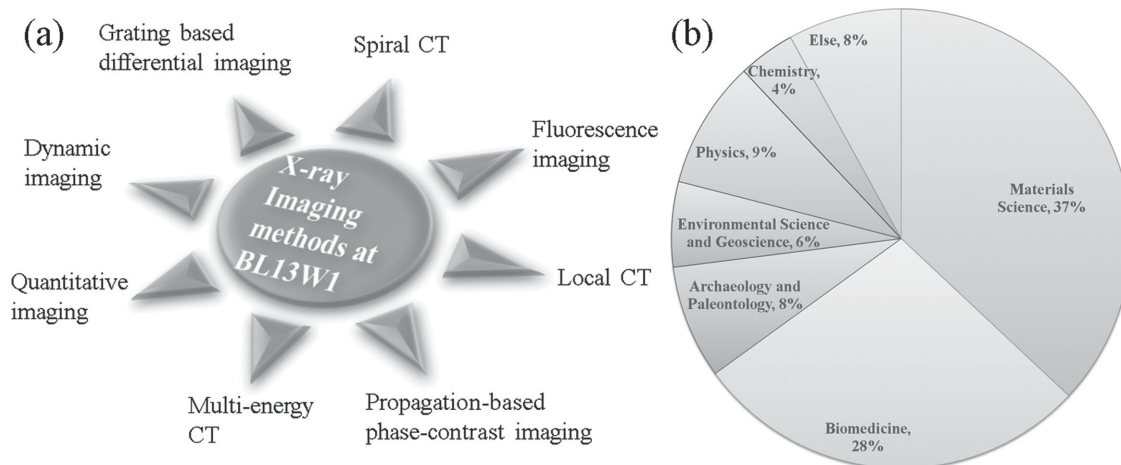


Figure 1. a) The X-ray imaging methods at BL13W1, b) statistics for user research fields at BL13W1

pro-osteogenesis and pro-angiogenesis to rapidly realize bone regeneration in vivo. Cai et al. investigated the in vivo effects of BMP-2/S-NP/G on the bone regeneration and vessel formation in the critical-sized defect of rabbit radius by SR- μ CT, histological analysis, immunohistochemistry, and biomechanical measurements.^[26] The results indicated that both controlled release of active BMP-2 and the favorable vascularization at the defect site contributed by BMP-2/S-NP/G played a crucial role in accelerating and promoting bone augmentation. Jiang et al. investigated the visualization of the three-dimensional structure of dermal tissue by SR- μ CT: the normal dermal tissues were found to consist of a network of elliptically shaped regions containing a web of fibre bundles.^[27]

The involvement of small vessels is very crucial pathologically in some major diseases. In vivo imaging of micro-vessels at early stages is an important step in understanding the development mechanism, early detection, and evaluation of therapeutic effects of both tumors and neurovascular diseases. At the BL13W1, ex vivo and in vivo micro-angiography using SR-imaging have been developed as powerful tools to study small vessels of tumors and neurovascular diseases. Liu et al. investigated physiological features of whole-body mouse microvasculature using barium sulfate as a contrast agent,^[28] and the 3D reconstruction of lung cancer angiogenesis with barium was obtained with a spatial resolution of about 10 μ m, which is much higher than that of conventional angiography.^[5] Yuan et al. developed a synchrotron radiation angiography technique to study vascular morphology in the suture middle cerebral artery occlusion model. Guan et al. observed hemodynamic changes after middle cerebral artery occlusion, and identified the physical properties of suture.^[29] Cai et al. visualized pathophysiological changes of small arteries in a saccular cerebral aneurysms animal model.^[30] Tang et al. introduced microbubbles into tissue, and the microbubbles produced a significant change in the refractive index and highlighted the lumen of the vessel. This investigation demonstrated that microbubble-based PPCI is a promising method to visualize the mouse renal vasculature and tumor-associated vessels using SR phase-contrast imaging.^[6]

However, in vivo phase-contrast imaging of blood vessels without a contrast agent is still a big challenge. If the intensity difference could be increased between the vessel wall and other surrounding soft tissues, then in vivo phase-contrast imaging of blood vessels may be achieved. It has been attempted to specifically target the endothelium of blood vessels with heavy-element nanoparticles. Liu et al. developed RGD peptide conjugated magnetite nanocluster probes for high-resolution micro-CT imaging of tumor angiogenesis, and angiogenic vessels were clearly detected by in vivo micro-CT imaging. It is particularly promising to realize in vivo SR phase-contrast imaging of blood vessels. Further investigations in synchrotron radiation phase-contrast imaging combined with targeted nanoparticle probes are being performed at the BL13W1 beamline of SSRF with the aim of visualizing vascular diseases of the brain and tumors in the near future.

2. Conclusions

SR-based imaging has attracted extensive attention especially when third generation SR facilities became available in the

1990s. SR-based imaging allows for high temporal resolution with high spatial resolution 3D imaging, which has broad applications in the research fields of materials and biomedical sciences. A number of X-ray imaging methods has been developed at the BL13W1 beamline driven by the user experimental needs since it was formally opened to users in May 2009. These developments have substantially increased the experimental efficiency and sample adaptability, which could be readily used in material, biomedical, and related investigations. In the coming years, dynamic micro-CT with a sub-second time scale, full-field nano-imaging with large field of view, and fast imaging ranging from 100 picoseconds to milliseconds are to be developed and opened to user experiments at SSRF.

Acknowledgements

This work was supported by the National Basic Research Program of China (grants 2010CB834300, 2010CB834301, and 2010CB834303), the CAS-CSIRO cooperation research project grant GJHZ1303, the National Natural Science Foundation of China (grants U1232205, 11375257, and 11275126).

Received: July 3, 2014

Revised: August 20, 2014

Published online: October 15, 2014

- [1] J. Baruchel, P. Bleuet, A. Bravin, P. Coan, E. Lima, A. Madsen, W. Ludwig, P. Pernot, J. Susini, *C. R. Phys.* **2008**, *9*, 624.
- [2] A. Bravin, P. Coan, P. Suortti, *Phys. Med. Biol.* **2013**, *58*, R1.
- [3] a) H. Xie, B. Deng, G. Du, Y. Fu, Y. He, H. Guo, G. Peng, Y. Xue, G. Zhou, Y. Ren, Y. Wang, R. Chen, Y. Tong, T. Xiao, *J. Instrum.* **2013**, *8*, C08003; b) T. Q. Xiao, H. L. Xie, B. Deng, G. H. Du, R. C. Chen, *Acta Optica Sinica* **2014**, *34*, 100001.
- [4] R. C. Chen, H. L. Xie, L. Rigon, R. Longo, E. Castelli, T. Q. Xiao, *Opt. Lett.* **2011**, *36*, 1719.
- [5] X. X. Liu, J. Zhao, J. Q. Sun, X. Gu, T. Q. Xiao, P. Liu, L. X. Xu, *Phys. Med. Biol.* **2010**, *55*, 2399.
- [6] R. B. Tang, Y. Xi, W. M. Chai, Y. T. Wang, Y. J. Guan, G. Y. Yang, H. L. Xie, K. M. Chen, *Phys. Med. Biol.* **2011**, *56*, 3503.
- [7] A. E. Hughes, A. Trinchin, F. F. Chen, Y. S. Yang, I. S. Cole, S. Sellaiyan, J. Carr, P. D. Lee, G. E. Thompson, T. Q. Xiao, *Adv. Mater.* **2014**, *26*, 4504.
- [8] T. Wang, J. Zhu, H. Kang, Z. Chen, Y. Fu, W. Huang, T. Xiao, *Appl. Phys. A* **2014**, *1*.
- [9] A. Momose, *Jpn. J. Appl. Phys.* **2005**, *44*, 6355.
- [10] S. W. Wilkins, T. E. Gureyev, D. Gao, A. Pogany, A. W. Stevenson, *Nature* **1996**, *384*, 335.
- [11] X. Wei, T. Q. Xiao, L. X. Liu, G. H. Du, M. Chen, Y. Y. Luo, H. J. Xu, *Phys. Med. Biol.* **2005**, *50*, 4277.
- [12] H. Q. Liu, Y. Q. Ren, H. Guo, Y. L. Xue, H. L. Xie, T. Q. Xiao, X. Z. Wu, *Chin. Opt. Lett.* **2012**, *10*, 121101.
- [13] Y. Q. Ren, C. Chen, R. C. Chen, G. Z. Zhou, Y. D. Wang, T. Q. Xiao, *Opt. Express* **2011**, *19*, 4170.
- [14] R. C. Chen, L. Rigon, R. Longo, *Opt. Express* **2013**, *21*, 7384.
- [15] a) J. C. Qi, Y. Q. Ren, G. H. Du, R. C. Chen, Y. D. Wang, Y. He, T. Q. Xiao, *Acta Optica Sinica*, **2013**, *33*, 1034001; b) Y. Xi, B. Q. Kou, H. H. Sun, J. C. Qi, J. Q. Sun, J. Mohr, M. Borner, J. Zhao, L. X. Xu, T. Q. Xiao, Y. J. Wang, *J. Synchrotron Radiat.* **2012**, *19*, 821.
- [16] Y. D. Wang, G. Y. Peng, Y. J. Tong, G. Z. Zhou, Y. Q. Ren, Q. Yang, T. Q. Xiao, *Acta Physica Sinica* **2012**, *61*, 174.

- [17] W. H. Chen, Y. D. Wang, H. Q. Liu, B. A. Deng, Y. S. Yang, T. Q. Xiao, *Chin Opt. Lett.* **2014**, 12, 023401.
- [18] R. C. Chen, R. Longo, L. Rigon, F. Zanconati, A. De Pellegrin, F. Arfelli, D. Dreossi, R. H. Menk, E. Vallazza, T. Q. Xiao, E. Castelli, *Phys. Med. Biol.* **2010**, 55, 4993.
- [19] L. L. Ye, Y. L. Xue, L. H. Ni, H. Tan, Y. D. Wang, T. Q. Xiao, *J. Instrum.* **2013**, 8, C07006.
- [20] Y. D. Wang, Y. S. Yang, I. Cole, A. Trinchì, T. Q. Xiao, *Corrosion* **2013**, 64, 180.
- [21] R. C. Chen, D. Dreossi, L. Mancini, R. Menk, L. Rigon, T. Q. Xiao, R. Longo, *J. Synchrotron Radiat.* **2012**, 19, 836.
- [22] Q. Yang, B. Deng, W. W. Lv, F. Shen, R. C. Chen, Y. D. Wang, G. H. Du, F. H. Yan, T. Q. Xiao, H. J. Xu, *J. Synchrotron Radiat.* **2012**, 19, 210.
- [23] X. F. Hu, L. B. Wang, F. Xu, T. Q. Xiao, Z. Zhang, *Carbon* **2014**, 67, 368.
- [24] Y. C. Li, F. Xu, X. F. Hu, D. Kang, T. Q. Xiao, X. P. Wu, *Acta Mater.* **2014**, 66, 293.
- [25] H. Zhou, X. H. Peng, E. Perfect, T. Q. Xiao, G. Y. Peng, *Geoderma* **2013**, 195, 23.
- [26] L. Cao, J. Wang, J. Hou, W. Xing, C. Liu, *Biomaterials* **2014**, 35, 684.
- [27] Y. Jiang, Y. Tong, S. Lu, *J. Tissue Eng. Regen. Med.* **2012**, DOI: 10.1002/term.1579.
- [28] P. Liu, J. Q. Sun, J. Zhao, X. X. Liu, X. Gu, J. Li, T. Q. Xiao, L. X. Xu, *J. Synchrotron Radiat.* **2010**, 17, 517.
- [29] Y. J. Guan, Y. T. Wang, F. L. Yuan, H. Y. Lu, Y. Q. Ren, T. Q. Xiao, K. M. Chen, D. A. Greenberg, K. L. Jin, G. Y. Yang, *Stroke* **2012**, 43, 888.
- [30] J. Cai, C. He, F. L. Yuan, L. J. Chen, F. Ling, *J. Clin. Neurosci.* **2012**, 19, 135.